

The morphology of polyvinylpyrrolidone nanofibers containing *Anredera cordifolia* leaves

Ida Sriyanti^{1*}, Muhammad Rama Almafie², Yuda Prasetya Nugraha³, Meutia Kamilatun Nuha Ap Idjan⁴, and Jaidan Jauhari⁵

^{1,2} Physics Education, Faculty of Education, Universitas Sriwijaya, Palembang, South Sumatera, Indonesia

³ Department of Pharmaceutics, School of Pharmacy, Institut Teknologi Bandung, Jalan Ganesa 10, Bandung, Indonesia

⁴ Department of Medical Education, Universitas Sriwijaya, Palembang, South Sumatera, Indonesia

^{1,2,4,5} Laboratory of Instrumentation and Nanotechnology Applications, Faculty of Computer Science, Universitas Sriwijaya, Palembang, South Sumatera, Indonesia

*Corresponding Address: ida_sriyanti@unsri.ac.id

Article Info

Article history:

Received: May 04, 2021

Accepted: September 05, 2021

Published: October 30, 2021

Keywords:

Electrospinning;
 Crystal;
 hydrogen bonds;
 Polyvinilpirolidon.

ABSTRACT

The electrospinning method has been used successfully to make polyvinylpyrrolidone nanofiber containing *Anredera cordifolia* leaves (BLE). The research methods used were qualitative and pure experiment method. Polyvinilpirolidone nanofibers containing BLE were prepared with three mass variations of the polyvinylpyrrolidone (% w/w), namely 12%, 10%, and 8% w/w, respectively. The results of the macroscopic photo show that the fiber structure looks white for PVP nanofibers and yellow for PVP/BLE nanofibers. The fiber morphology was analyzed using SEM and the results showed that PVP and all PVP/BLE nanofibers were like a continuous strand of crossbars with a diameter of 590 – 1190 nm. The decrease in the concentration of the PVP polymer led to a reduction in the diameter of the resulting nanofibers. The coefficients of variance (ϵ), of the PVP, BLE1, BLE2, and BLE3 nanofibers were 0.06, 0.09, 0.11, and 1.22, respectively. The physicochemical structure of the nanofibers was evaluated using XRD and FTIR. The chemical analysis (FTIR) showed that there was a molecular interaction between *Anredera cordifolia* leaves extract and polyvinylpyrrolidone in the form of hydrogen bonds. The physics analysis (XRD) shows the effect of the electrospinning process, which is to change the structure of BLE crystals to semi crystals. The application of PVP/BLE nanofiber for wounds dressing.

© 2021 Physics Education Department, UIN Raden Intan Lampung, Indonesia.

INTRODUCTION

The development of nanotechnology has changed the way in which technological advances are seen for each material is arranged at the atomic or molecular level. As a result, materials that have unique properties are superior to existing materials. A nanofiber is a form of nanostructures. The nanofibers are produced from the electrospinning method using high voltages through polymer mixing (Jauhari, et al., 2021; Watanabe et al., 2019). Moreover, the process is relatively easy and can produce large amounts of fiber in a relatively short

time (Nayak et al., 2017; Ramakrishna et al., 2010). Its simplicity and low cost can be applied on an industrial scale making the electrospinning method an economical alternative candidate for producing high-performance nanofibers for various applications, for example for medical applications such as drug delivery systems (Celebioglu & Uyar, 2020; Ozcan & Cagil, 2021), skin repair (Bellu et al., 2020), and wound dressings (Sriyanti et al., 2021). Furthermore, it can also be applied in the electronic field, such as electrodes and separators in supercapacitors (Fukuhara et

al., 2021; Jauhari, et al., 2021; Almafie, et al., 2021; Patel et al., 2020; Xu et al., 2020), and lithium batteries (An et al., 2019; Watanabe et al., 2019).

The advantages of nanofibrous with other materials are that it has extraordinary characteristics, namely having a small size, wide surface ratio, high amount of porosity, and flexibility when used for wound dressings. Mixing drugs into nanofiber can also increase the solubility of drugs that are difficult to dissolve, and the bioavailability of drugs, to increase the therapeutic effect and to reduce drug toxicity (Daghrery et al., 2020; Sriyanti et al., 2018).

Several studies have reported the advantages of nanofibers. Sriyanti (2018) reports that the incorporation of mangosteen in PVP nanofibers can increase the solubility and bioavailability of alpha mangosteen, as indicated by the increase in the release pattern. At the same, 5 minutes, PVP/mangosteen nanofibers release 49% while pure mangosteen is 13% (Sriyanti et al., 2018).

Recently, Sriyanti (2021) has reported that the effect of PVP/CA/ independent leaf nanofibers causes an increase in the release pattern of independent leaves. The initial release phase for independent leaves loaded in PVP/CA nanofibers is burst release, marked by the release of DOE in the PCP/CA fiber in a very short amount of time, the cumulative average COE released from the nanofiber is 35% at 5 minutes. The nanofibers also change the chrysanthemum phase of COE to become amorphous, thereby increasing the drug dissolution behavior (Sriyanti et al., 2021). Furthermore, the effect of the very high surface properties of the PVP/CA/DOE nanofiber makes the flavonoids from the COE released at a certain time higher to extinguish free radicals from outside more effectively than pure COE (Sriyanti et al., 2021).

Research on PVA/Honey loaded alginate nanofibers with active ingredients for antibacterial has also been carried out by other researchers (Tang et al., 2019). Besides

the field of medicine, the previous researcher, Jauhari (2021), also reported an increase in the electrochemical performance of graphene from oil palm shells which is included in PAN nanofiber for supercapacitor electrode applications (Jauhari, et al., 2021). The effect of the high surface area and small size of the rGOPKS/PAN nanofiber produced a high energy density (Jauhari, et al., 2021). However, evaluation of the morphological and physicochemical properties of PVP nanofibers/ *Anredera cordifolia* leaf extract is rare.

Materials that can be spun using the electrospinning technique can come from natural polymers and synthetic polymers. Polyvinylpyrrolidone (PVP) is a synthetic polymer that has been widely used in the pharmaceutical industry as an integrated tablet stabilizer and active substance carrier for antibacterial applications (Rac et al., 2019; Sriyanti et al., 2018). The use of PVP in the pharmaceutical field is supported by its hydrophilic, non-toxic, biodegradable, water-soluble, and also has good biocompatibility characteristics (Edikresnha et al., 2019; Sriyanti et al., 2017).

Anredera cordifolia leaves contain active compounds such as alkaloids, flavonoids, essential oils, saponins, and triterpenoids (Ramadhan, 2021; Ye et al., 2019). The flavonoid compounds in *Anredera cordifolia* leaves are useful as an antiseptic and antibacterial which is very useful for wounds. The mechanism of action of this compound is through the destruction of cell walls and deposition of cell proteins from microorganisms resulting in coagulation and malfunction of these microorganisms (Hermawan & Laksono, 2013). Potential pharmacological activities of *Anredera cordifolia* leaf extract have been proven in-vivo and in-vitro (Laksmiawati et al., 2017; Sakti et al., 2019).

In this study, PVP and *Anredera cordifolia* leaves extract were synthesized using a simple method, electrospinning. The morphology of polyvinylpyrrolidone

containing *Anredera cordifolia* leaves extract was evaluated using scanning electron microscope (SEM) observation. Analysis of physical and chemical properties was conducted using observations of functional groups, while analysis of intermolecular interactions was carried out using Fourier-transform infrared spectroscopy (FTIR). Meanwhile, investigations of changes in the crystal structure were conducted using X-ray diffraction (XRD).

METHODS

The research methods used for electrospun of PVP/BEL were qualitative and pure experiment methods.

1. Materials

The materials used for this study were Polyvinylpyrrolidone polymer with a molecular weight of 1,300,000 mol/kg obtained from Sigma Aldrich, 96% ethanol obtained from bratachem in Palembang (South Sumatera Province), and *Anredera cordifolia* leaves purchased from traditional markets in Palembang. The apparatus of electrospun PVP/BEL was Nanolab, Malaysia.

2. Preparation of *Anredera cordifolia* leaves Ekstrak

Anredera cordifolia leaves extract was made by maceration. The part of the *Anredera cordifolia* leaves was dried in the sun for a few days until the leaves were dry. Then, the dried leaves were chopped (cut into small pieces). *Anredera cordifolia* leaves that have been chopped were then added with 96% ethanol solvent. First, the *Anredera cordifolia* leaves, which had been chopped, were soaked in solvent for 73 hours and then stirred every day. The purpose of stirring was to homogenize the solution during the immersion process and accelerate the contact between the sample and the solvent (Khunaifi, 2010). This solvent might bind the active compounds presented in *Anredera cordifolia* leaves and carried by the solvent

through the filter, then collected in the collecting container. The more concentrated the liquid in the collection container indicates the presence of compounds that are bound and carried away by the solvent. This process was carried out continuously until the liquid in the collection container was completely clear, which indicates that there are no more compounds that can be bound by the solvent. The liquid collected in the collection container was then processed using a rotary evaporator with a temperature of 40°C to evaporate the solvent molecules until finally, *Anredera cordifolia* leaves extract was obtained in the form of a paste.

3. Synthesis of nanofiber

The nanofibers were made by dissolving 15% (w/w) polyvinylpyrrolidone (PVP) into ethanol as a precursor solution. Then, *an Anredera cordifolia* leaves extract (BLE) with a concentration of 2% (w/w) was added to the PVP solution. The variation used was the PVP concentration in % w/w. In order for the PVP and BLE solutions to be homogeneously composited, the solution was stirred using a magnetic stirrer (Bante MS400, China) with a rotational speed of 500 rpm, the temperature of 80°C, for 120 minutes. All variations of the PVP/BLE composite solution were labeled BLE1, BLE2, and BLE3, respectively. Table 1 is showing the details of variations in the PVP/BLE composite.

Table 1. The details of variations in the PVP/BLE composite

No	Sampel	PVP (% w/w)	BLE (% w/w)
1	PVP	12	0
2	BLE1	12	2
4	BLE2	10	2
5	BLE3	8	2

The polymer solution synthesis was electro-spun using electrospinning apparatus (Nanolab, malaysia) as illustrated in the schematic diagram in Figure 1. The composite PVP/BLE solution, which was homogeneous, was transferred to a 10 ml/cc

(Terumo, Philippines) with a needle length of 38 mm, the diameter of 21 Gauge. The process parameters were kept constant and the polymer was then dispensed by a syringe pump. Electrospinning parameters were used: flow rate 5 μl /minute, applied voltage at 14 kV, and tip-gap collector distance at 12 cm. The speed of the drum collector in the electrospinning device used a speed of 300 rpm. The apparatus was placed in a temperature and humidity-controlled room ($25 \pm 0.5^\circ\text{C}$, RH 55-65%).

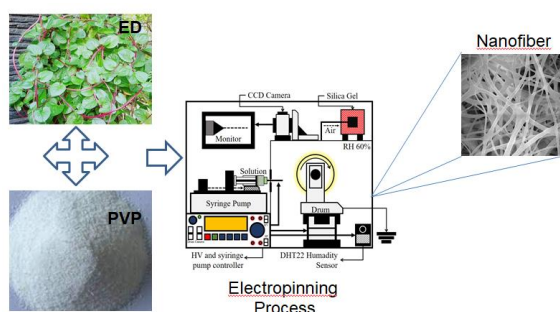


Figure 1. The schematic illustration of the experiment

4. The Characterization of PVP Nanofiber and PVP/ BLE Nanofibers

The morphology and distribution of the PVP, BLE1, BLE2, and BLE3 were observed using scanning electron microscopy (SEM) (Vega 3 Tescan, Japan). The voltage source used was 15 kV with a magnification of 10,000x. Meanwhile, analysis of fiber size used Image J1 1.52 A (Nasional Institutes of Health, USA), and to obtain fiber average data and fiber distribution Origin Pro 2018 was used (OriginLab Corporation, USA). The functional groups and intermolecular interactions of the PVP, BLE1, BLE2, and BLE3 nanofibers were observed using Fourier Transform Infrared Spectroscopy (FTIR) (Alpha II Bruker, Japan). The wavenumber used was in the range of 500-4000 cm^{-1} . Meanwhile, the identification of crystal structure changes and molecular interactions of PVP, BLE1, BLE2, and BLE3 were recorded using X-Ray Diffraction (Rigaku MiniFlex 600, Japan). The source of diffraction radiation comes from Sc 70 tube with a voltage of 30 kV, a current of 10 mA, and a pattern of 2θ with an angle of 5° to 80° .

RESULTS AND DISCUSSION

1. PVP/*Anredera cordifolia* leaves Nanofiber

The formation of the PVP/ BLE nanofiber was successfully carried out using the electrospinning method involving the same process parameters and environmental parameters for each spinning, namely a flow rate of 5 μl /minute, a voltage of 14 kV, and a tip-gap collector distance of 12 cm. The needle length was 38 mm with a diameter of 21 Gauge. Controlled temperature and humidity were $25 \pm 0.5^\circ\text{C}$, RH 40-50%. Figure 2 visualizes the macroscopic spinning of the PVP, BLE1, BLE2, and BLE3 nanofiber.

The observed structure of the nanofibers mats had fine characteristics such as tissue paper. Besides, the color of the fiber changes when BLE was inserted into the PVP nanofiber, white and yellow, shown in Figures 2b,2c, and 2d. This is because *Anredera cordifolia* leaves are extracted perfectly into the PVP nanofibers. This condition has also been reported by several previous studies (Pusporini et al., 2018; Sriyanti et al., 2020; Sriyanti et al., 2017, 2018, 2021). Meanwhile, the color changes and flexible structure of PVP nanofibers and PVP/*Anredera cordifolia* leaves nanofiber are shown in Figure 2.

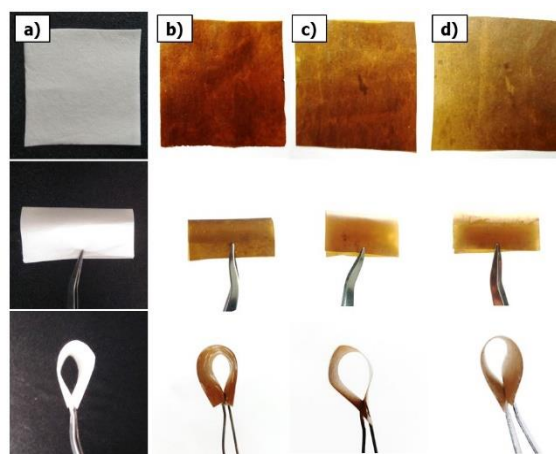


Figure 2. Nanofiber PVP/ BLE (a) PVP, (b) BLE1, (c) BLE2, dan (d) BLE3.

The formation of PVP and PVP/ *Anredera cordifolia* leaves nanofiber (BLE1, BLE2,

and BLE3) was influenced by three factors that work in the electrospinning system, namely (a) a high voltage; that causes an electric force in the solution, where a negative charge might move to the tip of the needle (Jauhari, et al., 2021; Almafie, et al., 2021; Lamura et al., 2021; Ramakrishna et al., 2010); (b) Syring pump; that might produce a driving force for the flow of the PVP or PVP/BLE polymer solution flow to drip on the tip of the needle; (c) surface tolerance of PVP or PVP/BLE; that is a force that can hold the solution from falling and can radiate towards the collector (Jauhari et al., 2019; Nayak et al., 2017). The existence of an equilibrium between the three factors above caused the polymer solution of the PVP or PVP/ BLE polymer to be attracted and form a Taylor cone (Jauhari et al., 2019; Ramakrishna et al., 2010). The electrospinning system is given a quite high voltage that exceeds the critical potential of the solution, the solution not only extends to form a Taylor cone but will form a polymer jet. The polymer solution will stretch and the solvent will evaporate. Finally, the PVP or PVP/BLE solution that will form on the collector surface is in the form of a solid (Almafie et al., 2020), as visualized in Figure 2.

2. Morphology and Size Distribution of PVP Nanofiber and PVP/BLE Nanofibers

The morphology and size distribution of PVP, BLE1, BLE2, and BLE3 nanofiber obtained using SEM with 1000 times magnification is shown in Figure 3. The resulting PVP and BLE morphology is a continuous strand of the strand that crosses each other and is free of beads. The variation of % w/w polyvinylpyrrolidone containing *Anredera cordifolia* leaves did not affect the shape of these fibers. The results of this experiment support a previous study that the addition of mangosteen peel extract in the fiber does not affect the shape of the nanofibers produced (Sriyanti et al., 2018).

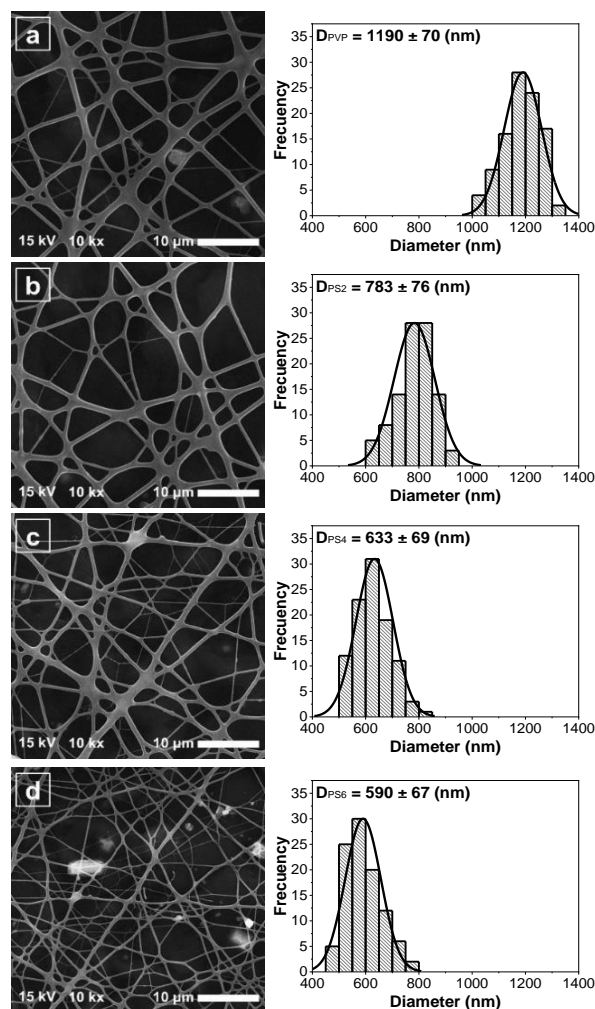


Figure 3. The Morfology and Diameter Distribution nanofibrous of (a) PVP, (b) BLE1, (c) BLE2, dan (d) BLE3.

The average diameter of PVP pure nanofiber without loading in *Anredera cordifolia* leaves extract (D_{BLE}) was 1190 nm with a standard deviation (σ_{PVP}) of 70 nm. The mean diameter (D_{BLE1}) and standard deviation (σ_{BLE1}) of the BLE1 nanofibers (12:2) were 783, and 76 nm, respectively. The diameter (D_{BLE2}) and standard deviation (σ_{BLE2}) of BLE2 nanofibers were 633 nm and 69 nm. At last, the average diameter (D_{BLE3}) and standard deviation (D_{BLE3}) of the BLE3 nanofiber were 590 and 67 nm. This indicates that the reduction of the PVP containing BLE from 12% to 8 % resulted in a decrease in the mean diameter of BLE fiber by 60%. Figure 4 shows the PVP construct (% w/w) on the mean diameter of the nanofibers.

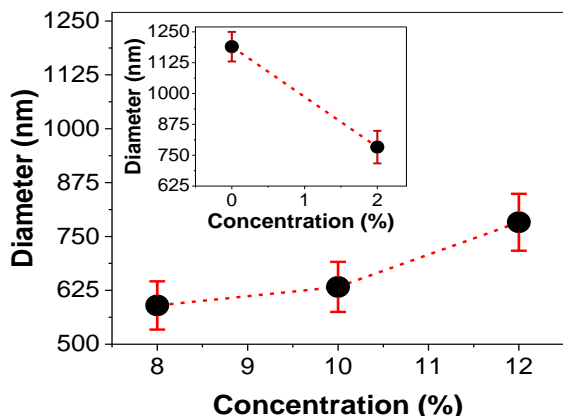


Figure 4. The effect of the concentration of PVP/BLE solution to the fiber diameter.

From the graph, it can be seen that the resulting nanofiber diameter shrinks as the PVP concentration decreases. This happens because of the effect of viscosity in the nanofiber solution (Ramakrishna et al., 2010; Sriyanti et al., 2020). The low viscosity causes the stretching process of the polymer solution to be lower in a strong and constant electric field (Singh et al., 2020). During electrospinning, a solution with a low solution viscosity has a low viscoelastic force, causing the electrostatic stretching force to be weaker (Tarus et al., 2016).

This process has a significant effect on the reduction in the size of the PVP/BLE nanofiber. Meanwhile, the increased concentration of the PVP/BLE solution increases the viscosity, causing an increase in the viscoelastic force. This allows the solvent molecules to be distributed over the entangled polymer molecules which leads to an increase in fiber diameter (Tarus et al., 2020; Tarus et al., 2016).

The coefficient of variance (ε), of the PVP, BLE1, BLE2, and BLE3 nanofibers were 0.06, 0.09, 0.11, and 1.22, respectively. These results indicate that the distribution of nanofibers is homogeneous because the value of ε was smaller than 0.3 (Almafie et al., 2020; Edikresnha et al., 2019; Sriyanti et al., 2017).

High voltage does not affect the jet balance or does not produce many side jets that enable the fiber diameter to be homogeneous (Almafie et al., 2020; Sriyanti et al., 2020). The high voltage might induce

the required charge on the solution along with the external electric field. Both have the effect of stretching in which, in this case, the voltage causes the coulomb force and electric field to be stronger in the jet. This has the effect of reducing fiber diameter and also encourages faster solvent evaporation to produce drier fibers (Abbas et al., 2016; Jauhari, Almafie, et al., 2021; Ramakrishna et al., 2010).

3. FTIR Analysis

FTIR Spectrum analysis was performed to identify the functional group characteristics of the PVP, BLE1, BLE2, and BLE3. The FTIR spectrum PVP/BLE is shown in Figure 5. The peaks of *Anredera cordifolia* leaves were recorded at 3331, 2971, 2879, 1646, 1380 cm^{-1} . The widening of the peak at 3331 cm^{-1} , 2871 cm^{-1} shows the O-H group stretching of the hydroxyl group (Rustanti & Fatmawati, 2020). The C-H stretching of the alkane group and the C=O stretching of the carbonyl group were shown by peaks at 2879 cm^{-1} and 1646 cm^{-1} (Rustanti & Fatmawati, 2020). This wave peak pattern confirms the presence of flavonoid chemical compounds in BLE (Rahma et al., 2016; Sriyanti et al., 2018).

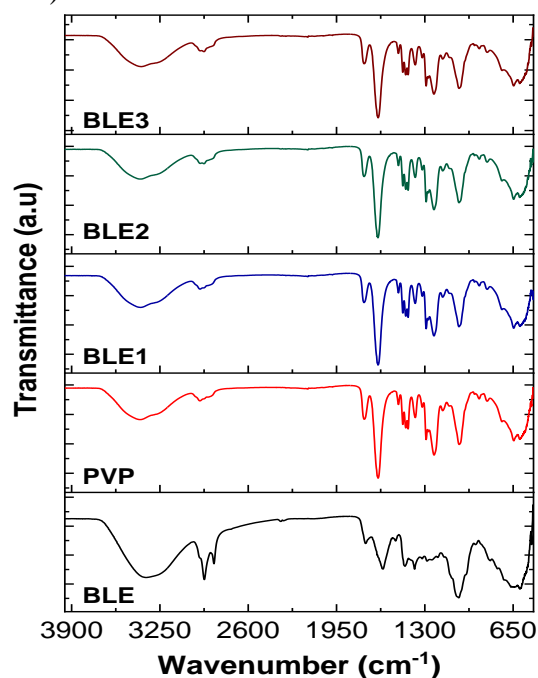


Figure 5. FTIR Spectrum of BLE, PVP and BLE1, BLE2, dan BLE3

On the other hand, the PVP FTIR spectrum showed a widening of the peak at 3391 cm^{-1} related to the hydroxyl group on O-H stretching vibration (López-Calderón et al., 2020). The peak at 2925 cm^{-1} shows the C-H Stretching bond of the alkane group (Sriyanti et al., 2017). A peak of 1650 cm^{-1} represents the C=O stretching of the carboxyl group and the peak of 1418 cm^{-1} indicates an aromatic group at C-C stretching (López-Calderón et al., 2020). The peak at 2925 cm^{-1} shows C-H stretching of alkane groups (Sriyanti et al., 2017).

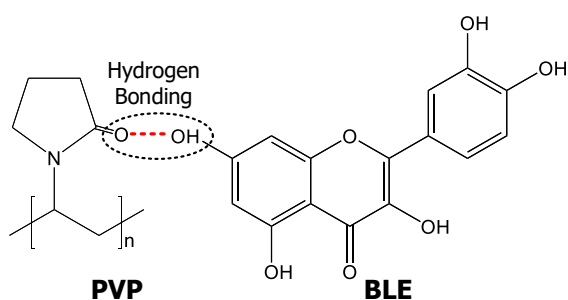


Figure 6. Hydrogen bonding between BLE dan PVP

The increase in PVP (% w/w) constellation containing *Anredera cordifolia* leaves resulted in several changes, namely: (1) BLE1; PVP wave number of 3395 cm^{-1} in the hydroxyl group (O-H) is shifted to be 3394 cm^{-1} , 3390 cm^{-1} for BLE2, and 3388 cm^{-1} for BLE3; (2), in the range of $1046\text{--}1040\text{ cm}^{-1}$, there was a decrease in the PVP wave number in the carboxyl group of the C=O, 1046 cm^{-1} to 1045 cm^{-1} in BLE1(12:2), to 1043 cm^{-1} in BLE 2, and 1044 cm^{-1} in BLE3 (8:2). Changes in wave number in hydroxyl (O-H) and PVP carbonyl groups containing *Anredera cordifolia* leaves (BLE1, BLE2, and BLE3) were caused by the interaction of molecules in *Anredera cordifolia* leaves extract with PVP molecules in the form of hydrogen bonds (Mulia et al., 2018; Sriyanti et al., 2017). Hydrogen bonds were formed due to O atoms bonding to H atoms. Figure 6 shows the Hydrogen bonding between *Anredera cordifolia* leaves extract (BLE) dan PVP. Thus, it can be concluded that the molecules of *Anredera cordifolia* leaf extract contained in polyvinylpyrrolidone (PVP)

strongly interact. This was supported by the results of the XRD analysis.

4. XRD Analysis

XRD analysis is a physics analysis used to study molecular interactions and changes in the crystal structure. Figure 7 displays XRD patterns of the PVP, BLE1, BLE2, and BLE3 composite nanofiber math. The crystal state of *Anredera cordifolia* leaves extract (BLE) is shown by a sharp peak at the 2θ position, 16.25° where this pattern represents flavonoid crystals (Rahma et al., 2016; Sriyanti et al., 2018). Meanwhile, the PVP diffraction patterns show two broad diffraction peaks peaking at the 2θ position namely 11.12° and 21.02° , indicating an amorphous structure.

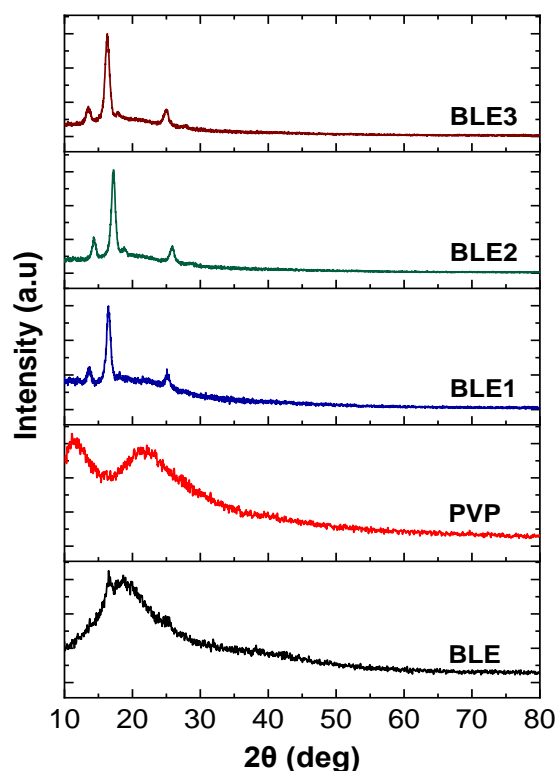


Figure 7. XRD patterns of BLE, PVP BLE1, BLE2, dan BLE3

After the PVP/BLE nanofiber composites formed a new diffraction pattern with the main peaks between $5\text{--}80^\circ$, there was a shift in the peaks in BLE1 (12:2), 14.35° and 16.93° . In BLE2(10:2) and BLE3(8:2), there were shifts in the peaks which increased

respectively, namely 14.72° , 17.21° , and 16.43° , 25.06° . The shifting of these peaks was caused by the electrospinning process (Sriyanti et al., 2021). This process causes a phase change of *Anredera cordifolia* leaves extract from semi-crystalline to crystalline.

CONCLUSION

PVP/BLE nanofiber had been successfully produced using the electrospinning method. Macroscopically, the electrospinning results of BLE1, BLE2, and BLE3 nanofibers had a homogeneous surface and are yellow in color. The formation of PVP and PVP fibers containing *Anredera cordifolia* leaves extract was influenced by high tension, syringe pump, and surface tension. Microscopically, SEM image analysis results show that all the resulting nanofibers look like continuous strands of strands that are crossed with each other and are free of beads. Decreasing the BLE concentration decreased the mean diameter size of the fibers. The diameter of the PVP (12:0), BLE1(12:2), BLE2(10:2), and BLE3(8:2) were 1190, 783, 633 dan 590 nm, respectively. The effect of the electrospinning process and the increase in the concentration of PVP containing BLE caused changes in the hydroxyl groups in the OH bonds (PVP: 1046 cm^{-1} , BLE1: 1046 cm^{-1} , BLE2: 1046 cm^{-1} , and BLE3: 1046 cm^{-1}) and the carboxyl groups in C=O bonds (PVP: 1046 cm^{-1} , BLE1: 1046 cm^{-1} , BLE2: 1046 cm^{-1} , and BLE3: 1046 cm^{-1}). There was a tendency to shift towards lower wavenumbers. This change in wavenumbers is seen as an interaction between BLE and PVP. During the electrospinning process, the BLE phase changes from a semicrystalline to a crystalline phase. PVP/BLE nanofiber can be applied to diabetic wound dressings

ACKNOWLEDGMENT

This research was financially supported by Dikti (Kemendikbud), Republic of Indonesia under the University's Excellence Research "PTUPT" Grant in the fiscal year 2021, No: 299/SP2H/LT/DRPM/2021.

REFERENCES

- Abbas, L. K., Jabur, A., & Muhi, S. M. (2016). Effects of high voltage and flow rate parameters on nanofibers diameter synthesis by electrospinning technique. *Journal of Physical Science and Application*, 6(1), 2159–5348. <https://doi.org/10.17265/2159-5348/2016.01.029>
- Almafie, M. R., Nawawi, Z., Jauhari, J., & Sriyanti, I. (2020). Electrospun of poly (vinyl alcohol)/ potassium hydroxide (PVA/KOH) nanofiber composites using the electrospinning method. *IOP Conference Series: Materials Science and Engineering*, 850, 012051. <https://doi.org/10.1088/1757-899X/850/1/012051>
- Ambekar, R. S., & Kandasubramanian, B. (2019). Advancements in nanofibers for wound dressing: A review. *European Polymer Journal*, 117, 304–336. <https://doi.org/10.1016/j.eurpolymj.2019.05.020>
- An, D., Shen, L., Lei, D., Wang, L., Ye, H., Li, B., Kang, F., & He, Y. B. (2019). An ultrathin and continuous Li₄ Ti₅O₁₂ coated carbon nanofiber interlayer for high rate lithium sulfur battery. *Journal of Energy Chemistry*, 31, 19–26. <https://doi.org/10.1016/j.jechem.2018.05.002>
- Bellu, E., Garroni, G., Cruciani, S., Balzano, F., Serra, D., Satta, R., Montesu, M. A., Fadda, A., Mulas, M., Sarais, G., Bandiera, P., Torreggiani, E., Martini, F., Tognon, M., Ventura, C., Beznoska, J., Amler, E., & Maioli, M. (2020). Smart nanofibers with natural extracts prevent senescence patterning in a dynamic cell culture model of human skin. *Cells*, 9(12), 3–15. <https://doi.org/10.3390/cells9122530>
- Celebioglu, A., & Uyar, T. (2020). Hydrocortisone/cyclodextrin complex electrospun nanofibers for a fast-dissolving oral drug delivery system. *RSC Medicinal Chemistry*, 11(2), 245–258.

- <https://doi.org/10.1039/c9md00390h>
- Daghrery, A., Aytac, Z., Dubey, N., Mei, L., Schwendeman, A., & Bottino, M. C. (2020). Electrospinning of dexamethasone/cyclodextrin inclusion complex polymer fibers for dental pulp therapy. *Colloids and Surfaces B: Biointerfaces*, 191(1), 111011. <https://doi.org/10.1016/j.colsurfb.2020.111011>
- Edikresnha, D., Suciati, T., Munir, M. M., & Khairurrijal, K. (2019). Polyvinylpyrrolidone/cellulose acetate electrospun composite nanofibres loaded by glycerine and garlic extract with: In vitro antibacterial activity and release behaviour test. *RSC Advances*, 9(45), 26351–26363. <https://doi.org/10.1039/c9ra04072b>
- Fukuhara, M., Kuroda, T., Hasegawa, F., Hashida, T., Takeda, M., Fujima, N., Morita, M., & Nakatani, T. (2021). Amorphous cellulose nanofiber supercapacitors. *Scientific Reports*, 11(1), 6436. <https://doi.org/10.1038/s41598-021-85901-3>
- Jauhari, J., Almafie, M. R., Annisa, M., Mataram, A., Marlina, L., Idjan, M. K. N. A., & Sriyanti, I. (2021). The morphology and scaling law model of polyvinylidene fluoride/carbon fiber using electrospinning technique. *Journal of Physics: Conference Series*, 1796(1), 012076. <https://doi.org/10.1088/1742-6596/1796/1/012076>
- Jauhari, J., Aj, S., Nawawi, Z., & Sriyanti, I. (2021). Synthesis and characteristics of polyacrylonitrile (PAN) nanofiber membrane using electrospinning method. *Journal of Chemical Technology and Metallurgy*, 56(4), 698–703.
- Jauhari, J., Almafie, M. R., Marlina, L., Nawawi, Z., & Sriyanti, I. (2021). Physicochemical properties and performance of graphene oxide/polyacrylonitrile composite fibers as supercapacitor electrode materials. *RSC Advances*, 11(19), 11233–11243. <https://doi.org/10.1039/d0ra10257a>
- Jauhari, J., Wiranata, S., Rahma, A., Nawawi, Z., & Sriyanti, I. (2019). Polyvinylpyrrolidone/cellulose acetate nanofibers synthesized using electrospinning method and their characteristics. *Materials Research Express*, 6(6), 064002. <https://doi.org/10.1088/2053-1591/ab0b11>
- Kalantari, K., Afifi, A. M., Jahangirian, H., & Webster, T. J. (2019). Biomedical applications of chitosan electrospun nanofibers as a green polymer – Review. *Carbohydrate Polymers*, 207, 588–600. <https://doi.org/10.1016/j.carbpol.2018.12.011>
- Laksmitawati, D. R., Widyastuti, A., Karami, N., Afifah, E., Rihibiha, D. D., Nufus, H., & Widowati, W. (2017). Anti-inflammatory effects of Anredera cordifolia and piper crocatum extracts on lipopolysaccharide-stimulated macrophage cell line. *Bangladesh Journal of Pharmacology*, 12(1), 35–40. <https://doi.org/10.3329/bjp.v12i1.28714>
- Lamura, M. D. P., Pulungan, M. A., Jauhari, J., & Sriyanti, I. (2021). The influence of control parameter on the morphology polyethersulfone/polyacrylonitrile (PES/PAN) fiber using electrospinning technique. *IOP Conference Series: Earth and Environmental Science*, 1796(1), 012084. <https://doi.org/10.1088/1742-6596/1796/1/012084>
- López-Calderón, H. D., Avilés-Arnaut, H., Galán-Wong, L. J., Almaguer-Cantú, V., Laguna-Camacho, J. R., Calderón-Ramón, C., Escalante-Martínez, J. E., & Arévalo-Niño, K. (2020). Electrospun polyvinylpyrrolidone-gelatin and cellulose acetate bi-layer scaffold loaded with gentamicin as possible wound dressing. *Polymers*, 12(10), 1–

12.
<https://doi.org/10.3390/polym12102311>
- Mulia, K., Krisanti, E. A., & Andika, G. (2018). Betain and alcohol-based deep eutectic solvents for vitexin extraction from binahong (*Anredera cordifolia*) leaves. *ASEAN Journal of Chemical Engineering*, 18(2), 1–6. <https://doi.org/10.22146/ajche.49530>
- Nayak, R., Padhye, R., & Arnold, L. (2017). Melt-electrospinning of nanofibers. In M. B. T.-E. N. Afshari (Ed.), *Electrospun Nanofibers* (pp. 11–40). Woodhead Publishing. <https://doi.org/10.1016/B978-0-08-100907-9.00002-7>
- Ozcan, F., & Cagil, E. M. (2021). Design and characterization of pH stimuli-responsive nanofiber drug delivery system: The promising targeted carriers for tumor therapy. *Journal of Applied Polymer Science*, 138(11), 50041. <https://doi.org/https://doi.org/10.1002/app.50041>
- Patel, A., Wilcox, K., Li, Z., George, I., Juneja, R., Lollar, C., Lazar, S., Grunlan, J., Grunlan, J., Tenhaeff, W. E., Lutkenhaus, J. L., & Lutkenhaus, J. L. (2020). High modulus, thermally stable, and self-extinguishing aramid nanofiber separators. *ACS Applied Materials and Interfaces*, 12(23), 25756–25766. <https://doi.org/10.1021/acsami.0c03671>
- Pusporini, P., Edikresnha, D., Sriyanti, I., Suciati, T., Munir, M. M., & Khairurrijal, K. (2018). Electrospun polyvinylpyrrolidone (PVP)/green tea extract composite nanofiber mats and their antioxidant activities. *Materials Research Express*, 5(5), 054001. <https://doi.org/10.1088/2053-1591/aac1e6>
- Rac, V., Lević, S., Balanč, B., Olalde Graells, B., & Bijelić, G. (2019). PVA Cryogel as model hydrogel for iontophoretic transdermal drug delivery investigations. Comparison with PAA/PVA and PAA/PVP interpenetrating networks. *Colloids and Surfaces B: Biointerfaces*, 180(1), 441–448. <https://doi.org/10.1016/j.colsurfb.2019.05.017>
- Rahma, A., Munir, M. M., Khairurrijal, Prasetyo, A., Suendo, V., & Rachmawati, H. (2016). Intermolecular interactions and the release pattern of electrospun curcumin-polyvinylpyrrolidone fiber. *Biological and Pharmaceutical Bulletin*, 39(2), 163–173. <https://doi.org/10.1248/bpb.b15-00391>
- Ramadhan, A. (2021). The effectiveness of binahong (*anredera cordifolia* (ten.) steenis) extract in promoting fertility in male wistar rats after exposure to cigarette smoke. *Open Access Macedonian Journal of Medical Sciences*, 9(1), 123–128. <https://doi.org/10.3889/oamjms.2021.5881>
- Ramakrishna, S., Fujihara, K., Teo, W.-E., Lim, T.-C., & Ma, Z. (2010). An introduction to electrospinning and nanofibers. In *An Introduction to Electrospinning and Nanofibers*. <https://doi.org/10.1142/9789812567611>
- Rustanti, E., & Fatmawati, Z. (2020). The active compound of soursop leaf extract (*Annona muricata*, L.) as anti-vaginal discharge (*Fluor albus*). *IOP Conference Series: Earth and Environmental Science*, 456(1), 012071. <https://doi.org/10.1088/1755-1315/456/1/012071>
- Sakti, D. S., Haresmita, P. P., Yuniarti, N., & Wahyuono, S. (2019). Phagocytosis Activity of binahong (*anredera cordifolia* (tenore.) steenis) from secang, magelang, central java, Indonesia. *Journal of Pharmaceutical Sciences and Community*, 16(1), 7–13. <https://doi.org/10.24071/jpsc.001693>
- Sriyanti, I., Marlina, L., & Jauhari, J. (2020). Optimization of the electrospinning process for preparation of nanofibers from poly (vinyl alcohol) (PVA) and

- chromolaena odorata l. extrac (COE). *Jurnal Pendidikan Fisika Indonesia*, 16(1), 47–56. <https://doi.org/10.15294/jpfi.v16i1.12629>
- Sriyanti, I, Agustini, M. P., Jauhari, J., Sukemi, S., & Nawawi, Z. (2020). Electrospun nylon-6 nanofibers and their characteristics. *Jurnal Ilmiah Pendidikan Fisika Al-Biruni*, 9(1), 9–19. <https://doi.org/10.24042/jipfalbiruni.v9i1.5747>
- Sriyanti, I, Edikresnha, D., Rahma, A., Munir, M. M., Rachmawati, H., & Khairurrijal, K. (2017). Correlation between structures and antioxidant activities of polyvinylpyrrolidone/garcinia mangostana l. extract composite nanofiber mats prepared using electrospinning. *Journal of Nanomaterials*, 2017(1), 1–10. <https://doi.org/10.1155/2017/9687896>
- Sriyanti, I, Edikresnha, D., Rahma, A., Munir, M. M., Rachmawati, H., & Khairurrijal, K. (2018). Mangosteen pericarp extract embedded in electrospun PVP nanofiber mats: Physicochemical properties and release mechanism of α -mangostin. *International Journal of Nanomedicine*, 13(1), 4927–4941. <https://doi.org/10.2147/IJN.S167670>
- Sriyanti, I, Marlina, L., Fudholi, A., Marsela, S., & Jauhari, J. (2021). Physicochemical properties and In vitro evaluation studies of polyvinylpyrrolidone/cellulose acetate composite nanofibres loaded with Chromolaena odorata (L) King extract. *Journal of Materials Research and Technology*, 12, 333–342. <https://doi.org/https://doi.org/10.1016/j.jmrt.2021.02.083>
- Tang, Y., Lan, X., Liang, C., Zhong, Z., Xie, R., Zhou, Y., Miao, X., Wang, H., & Wang, W. (2019). Honey loaded alginate/PVA nanofibrous membrane as potential bioactive wound dressing. *Carbohydrate Polymers*, 219(1), 113–120. <https://doi.org/10.1016/j.carbpol.2019.05.004>
- Watanabe, T., Inafune, Y., Tanaka, M., Mochizuki, Y., Matsumoto, F., & Kawakami, H. (2019). Development of all-solid-state battery based on lithium ion conductive polymer nanofiber framework. *Journal of Power Sources*, 423(1), 255–262. <https://doi.org/10.1016/j.jpowsour.2019.03.066>
- Xu, J., Liu, Z., Zhang, F., Tao, J., Shen, L., & Zhang, X. (2020). Bacterial cellulose-derived carbon nanofibers as both anode and cathode for hybrid sodium ion capacitor. *RSC Advances*, 10(13), 7780–7790. <https://doi.org/10.1039/c9ra10225f>
- Ye, K., Kuang, H., You, Z., Morsi, Y., & Mo, X. (2019). Electrospun nanofibers for tissue engineering with drug loading and release. *Pharmaceutics*, 11(4). <https://doi.org/10.3390/pharmaceutics11040182>